

Supporting Information

Direct Spectroscopic Evidence for an $n \rightarrow \pi^*$ Interaction

*Santosh K. Singh, Kamal K. Mishra, Neha Sharma, and Alope Das**

anie_201511925_sm_miscellaneous_information.pdf

Supporting Information

Table of content

Contents

1. Experimental and computational methods	3
2. Table S1	4
3. Table S2	5
4. Figure S1	6
5. Table S3	7
6. Table S4	8
7. Table S5	8
8. Figure S2	9
9. Figure S3	10
10. Figure S4	11
11. Figure S5	12
12. Explanation of detail NBO analysis	12-14

1. Experimental and Computational Methods

Materials. Phenyl formate (purity $\geq 98.0\%$) was purchased from Sigma-Aldrich and used without further purification.

One-color resonant 2-photon ionization (1C-R2PI) spectroscopy. Electronic spectrum of phenyl formate was measured using 1C-R2PI spectroscopy in a home-built jet-cooled Time of Flight mass spectrometer. The details of the experimental setup have been described elsewhere.^[1] Here only a brief description has been provided. Vapor of phenyl formate produced by heating at 60°C was seeded in 70% Ne/30% He gas mixture and expanded into a high vacuum chamber through a pulsed nozzle (0.5 mm dia, 10 Hz, General valve, series 9). Jet-cooled molecular beam of phenyl formate was ionized using frequency doubled output of a tunable dye laser (10 Hz, ns, ND 6000, Continuum) pumped by second harmonic output of a Nd:YAG laser (10 Hz, ns, Surelite II-10, Continuum). In 1C-R2PI technique, the first photon at a certain wavelength electronically excites the molecules to one of the vibronic levels in the S_1 state and subsequently another photon of same wavelength ionizes the molecules. The ions are mass analyzed in the Time of Flight mass spectrometer.

UV-UV hole-burning spectroscopy. The presence of multiple conformers of phenyl formate in the experiment was determined using this technique. Here a UV probe laser (dye laser, 10 ns, 10 Hz, ND6000, Continuum, 200 $\mu\text{J}/\text{pulse}$) was fixed to a particular transition in the R2PI (electronic) spectrum and another UV pump laser (dye laser, 10 ns, 10 Hz, ND6000, Continuum, 400 $\mu\text{J}/\text{pulse}$) fired about 100 ns prior to the probe laser was scanned through the whole R2PI spectral region of the molecule. The pump and probe laser beams were spatially overlapped in the interaction region with the molecular beam. The hole-burning spectrum represents depletion in the probe ion signal for the transitions which belong to the same ground state conformer.

Resonant ion-dip infrared (RIDIR) spectroscopy. In this technique, a UV laser (dye laser, 10 ns, 10 Hz, ND6000, Continuum) was fixed to a particular transition in the R2PI spectrum and a tunable IR laser (resolution $\sim 2\text{ cm}^{-1}$, OPO/OPA, Laser Vision), pumped by a Nd:YAG laser (10 Hz, ns, Surelite II-10, Continuum) and fired 100 ns prior to the UV laser, was scanned through the carbonyl stretching region. The RIDIR spectrum shows depletion in the UV ion signal whenever the IR laser frequency matches with any vibrational transition in the molecule.

Quantum Chemistry calculations. Geometry optimizations and vibrational frequency calculations of different conformers of phenyl formate were performed using Gaussian09 package^[2]. Ground state (S_0) calculations were done at the M05-2X/aug-cc-pVDZ level while S_1 state calculations were done at the CIS/6-31+G(d) level of theory. Natural bond orbital (NBO) analysis was performed using the NBO program available in the Gaussian 09 software.^[3]

Table S1. Observed and calculated S_1 state vibrational frequencies (in cm^{-1}) of the cis and trans conformers of phenyl formate. S_1 state vibrational frequencies are calculated at the CIS/6-31+G(d) level of theory

cis conformer				trans conformer			
Obs. ^a	Calc.	Assignment	Description	Obs. ^b	Calc.	Assignment	Description
0.0		0_0^0		0.0		0_0^0	
43	46	39_0^1	Ph-O Torsion	39			
83		39_0^2		51	56	39_0^1	Ph-O Torsion
120		39_0^3		79			
145	137	38_0^1	Ring bend (boat)+C-O-C bend		110		O-CO torsion
157		39_0^4		126	134	37_0^1	Ring bend
179		$38_0^1 39_0^1$		171		$39_0^1 37_0^1$	
195	197	$37_0^1 / 39_0^5$	Ring Twist + O-CO torsion	204	208	36_0^1	Ring bend (boat)+Ph- O torsion
218	220	$36_0^1 / 38_0^1 39_0^2$	Ring Twist				
241		39_0^6					
261	259	$35_0^1 / 38_0^1 39_0^3$	Ring bend (boat) + O-CO torsion				
282		39_0^7					
302		$38_0^1 39_0^4$					
324		39_0^8					
335		$36_0^1 39_0^3$					
340		$38_0^1 39_0^5$					
348		$35_0^1 39_0^2$					
362		39_0^9					
376	373	34_0^1	Ring bend (chair)				
383		$38_0^1 39_0^6$					
397		39_0^{10}					
414		$34_0^1 39_0^1$					

^aRelative to the 0_0^0 band observed at 37590 cm^{-1} . ^bRelative to the 0_0^0 band observed at 37487 cm^{-1} . Mulliken notation has been followed to number the vibrational modes.

Table S2. A few selected geometrical parameters of the cis and trans conformers of phenyl formate in the S_0 and S_1 states. The structures in the S_0 state have been calculated at the M05-2X/aug-cc-pVDZ level of theory while the S_1 state structures have been calculated at the CIS/6-31+G(d) level of theory

	cis conformer		trans conformer	
	S_0	S_1	S_0	S_1
$r_{C=O}$ (Å)	1.20	1.18	1.19	1.17
$r_{C_{13}-H_{14}}$ (Å)	1.10	1.082	1.10	1.085
$d_{C=O \cdots \text{Ring center}}$ (Å)	3.75	3.91	-	-
$d_{H_{14} \cdots \text{Ring center}}$ (Å)	-	-	3.41	3.50
$a\theta$	48°	35°	-	-
$\angle C_3-O_{12}-C_{13}$	118°	124°	117°	120°
$\angle O_{12}-C_{13}-O_{15}$	126°	127°	122°	122°
$^b\angle C_3-O_{12}-C_{13}-O_{15}$	-0.04°	-3°	175°	171°
$^c\angle C_4-C_3-O_{12}-C_{13}$	-57°	-40°	-56°	-53°

$^a\theta$ is the angle between the plane containing the carbonyl oxygen atom and the aromatic plane; $^b\angle C_3-O_{12}-C_{13}-O_{15}$: O-CO torsional angle; $^c\angle C_4-C_3-O_{12}-C_{13}$: Ph-O torsional angle.

Table S2 lists a few selected geometrical parameters of the two conformers of phenyl formate, which support the observed IR spectroscopy results in terms of the presence of the $n \rightarrow \pi^*$ interaction. The lengthening of the C=O bond by 0.01 Å in the cis conformer compared to that in the trans conformer of phenyl formate is in line with the observed red-shift in the C=O stretching frequency in the cis conformer. It is interesting to note that the distance (3.75 Å) between the carbonyl oxygen and aromatic ring centroid ($d_{C=O \cdots \text{Ring center}}$) and the angle (48°) between the plane containing carbonyl oxygen and aromatic plane (θ) in the cis conformer of phenyl formate provided are in the acceptable range of the $n \rightarrow \pi^*$ interaction. Typical Burgi-Dunitz parameters i.e. $X \cdots C=O$ distance and $\angle X \cdots C=O$ for the $X \cdots C=O$ interaction are ≤ 3.2 Å and $109 \pm 10^\circ$, respectively while the similar parameters i.e. $X \cdots \pi_{\text{aromatic}}$ (centroid) distance and the angle (θ) between the plane containing X atom and aromatic plane for the $X \cdots \pi_{\text{aromatic}}$ interaction are 2.8 – 3.8 Å and $\leq 90^\circ$, respectively.

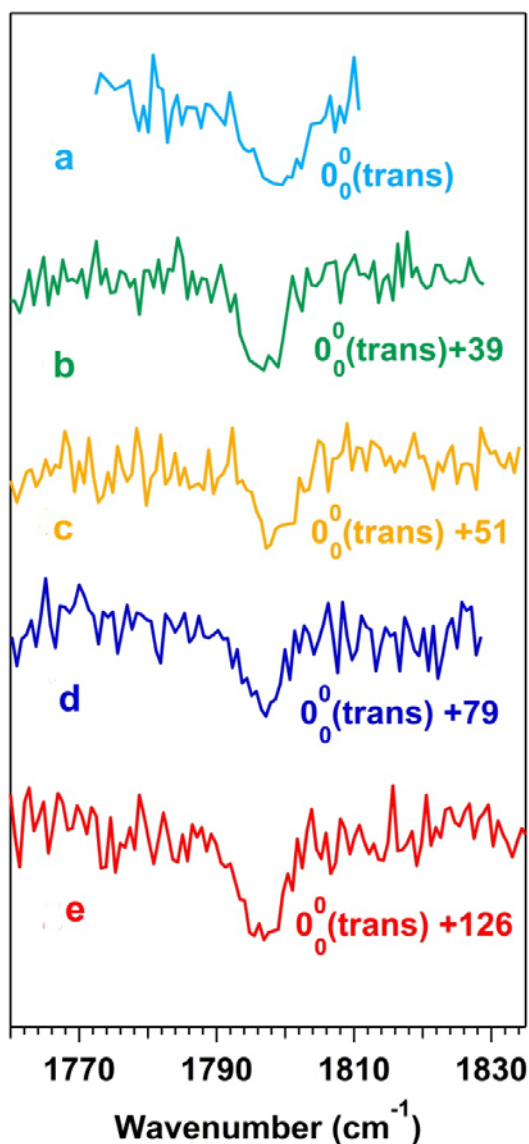


Fig. S1. IR spectra measured in the carbonyl stretching region by exciting the (a) 0_0^0 (trans), (b) 0_0^0 (trans) + 39 cm^{-1} , (c) 0_0^0 (trans) + 51 cm^{-1} , (d) 0_0^0 (trans) + 79 cm^{-1} and (e) 0_0^0 (trans) + 126 cm^{-1} bands of the electronic spectrum of phenyl formate shown in Fig. 1(c).

RIDIR spectra in parts (b) and (d) of Fig. S1 by excitation of bands A_1 and A_2 i.e. 0_0^0 (trans) + 39 cm^{-1} and 0_0^0 (trans) + 79 cm^{-1} bands in the electronic spectrum depicted in Figure 1(c) in the main text show C=O stretching frequency at 1797 cm^{-1} . Similar IR spectra have been obtained for excitation of all the electronic bands of the trans conformer of phenyl formate. Thus it is reconfirmed that the electronic bands marked as A_1 and A_2 in Fig. 1(c) in the main text originate due to the electronic transitions of the trans conformer of phenyl formate only.

Table S3. Second order perturbative energy ($E_{i \rightarrow j}^{(2)}$) values for interaction between various donor and acceptor NBOs in the cis and trans conformers of phenyl formate calculated at the M05-2X/cc-pVTZ level of theory

Interaction ^a	cis			trans		
	Donor (i)	Acceptor (j*)	$E_{i \rightarrow j}^{(2)}$ (kcal/mol)	Donor (i)	Acceptor (j*)	$E_{i \rightarrow j}^{(2)}$ (kcal/mol)
R ₁	O ₁₂ (n _p)	C ₁₃ =O ₁₅ (π^*)	49.45	O ₁₂ (n _p)	C ₁₃ =O ₁₅ (π^*)	43.11
	O ₁₂ (n _{σ})	C ₁₃ =O ₁₅ (σ^*)	7.66	O ₁₂ (n _{σ})	C ₁₃ =O ₁₅ (σ^*)	3.08
R ₂	O ₁₅ (n _p)	O ₁₂ -C ₁₃ (σ^*)	42.15	O ₁₅ (n _p)	O ₁₂ -C ₁₃ (σ^*)	43.49
	O ₁₅ (n _{σ})	O ₁₂ -C ₁₃ (σ^*)	1.28	O ₁₅ (n _{σ})	O ₁₂ -C ₁₃ (σ^*)	1.25
R ₃	O ₁₂ (n _p)	C ₂ =C ₃ (π^*)	10.13	O ₁₂ (n _p)	C ₃ =C ₄ (π^*)	10.45
	O ₁₂ (n _{σ})	C ₃ =C ₄ (σ^*)	4.84	O ₁₂ (n _{σ})	C ₃ =C ₄ (σ^*)	4.91
	O ₁₂ (n _{σ})	C ₂ =C ₃ (π^*)	3.95	O ₁₂ (n _{σ})	C ₃ =C ₄ (π^*)	4.40
	O ₁₂ (n _p)	C ₂ =C ₃ (σ^*)	3.78	O ₁₂ (n _p)	C ₃ =C ₄ (σ^*)	4.31
	O ₁₂ (n _p)	C ₃ =C ₄ (σ^*)	3.89	O ₁₂ (n _p)	C ₂ =C ₃ (σ^*)	4.69
R ₄	O ₁₅ (n _p)	C ₂ =C ₃ (π^*)	0.52	-	-	-
	O ₁₅ (n _p)	C ₄ =C ₅ (π^*)	0.51	-	-	-

^aR₁ interaction denotes the overlap between the lone pair orbitals (p-type and σ type) on the ether oxygen (O₁₂) and carbonyl π^* orbital. This interaction reduces the carbonyl stretching frequency.

^aR₂ interaction stands for the overlap between the lone pair orbitals (p-type and σ type) on carbonyl oxygen (O₁₅) and the σ^* orbital of the O₁₂-C₁₃ bond. This interaction increases the carbonyl stretching frequency or strengthen the C=O bond.

^aR₃ interaction denotes the overlap between the lone pair orbitals (p-type and σ type) on the ether oxygen (O₁₂) and the π^* and σ^* orbitals of the phenyl ring. This interaction tends to oppose the R₁ interaction i.e. increase the C=O stretching frequency.

R₄ interaction denotes the $n \rightarrow \pi^*$ interaction which involves overlap of lone pair orbital of carbonyl oxygen (O₁₅) and π^* orbitals of phenyl ring

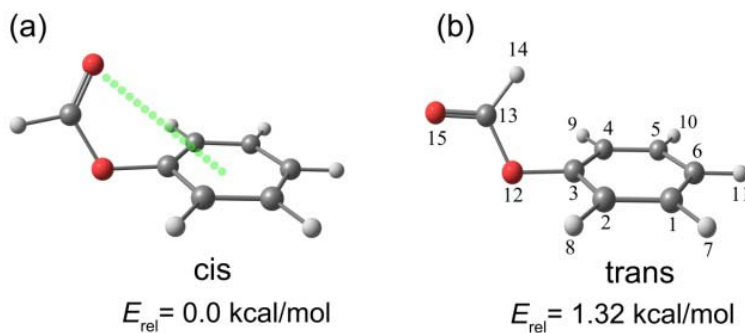


Table S4. Sum of multiple contributions of second order perturbative energy ($E_{i \rightarrow j}^{(2)}$) values for each of the R₁, R₂, R₃ and R₄ interactions in the cis and trans conformers of phenyl formate^b

Interaction	cis	trans
	Total $E_{i \rightarrow j}^{(2)}$ (kcal/mol)	Total $E_{i \rightarrow j}^{(2)}$ (kcal/mol)
R ₁	57.11	46.19
R ₂	43.43	44.74
R ₃	26.6	28.75
R ₄	1.03	-

^bR₁, R₂, R₃ and R₄ are defined at the footnote of Table S3.

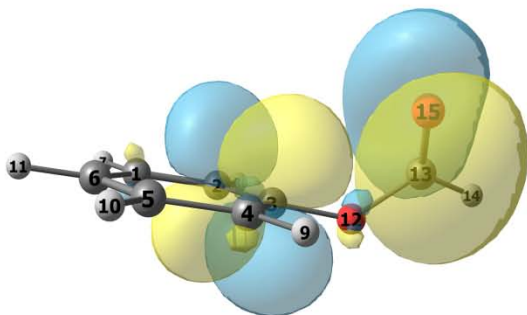
Table S5. Occupancy of the carbonyl oxygen O₁₅ lone pair electrons (p-type) of the cis conformer of phenyl formate on deletion of specific interaction(s)^c by performing NBO deletion analysis

Interactions		Occupancy of O ₁₅ (n _p) lone pair orbital
Case I	R ₁ , R ₂ , R ₃ , R ₄ (Not deleted)	1.84426
	R ₁ , R ₂ , R ₃ (Not deleted)	1.84501
	R ₄ (deleted)	
Case II	R ₁ , R ₃ (Not deleted)	1.93023
	R ₂ , R ₄ (deleted)	
	R ₁ , R ₃ , R ₄ (Not deleted)	1.92841
	R ₂ (deleted)	

^cR₁, R₂, R₃ and R₄ are defined at the footnote of Table S3.

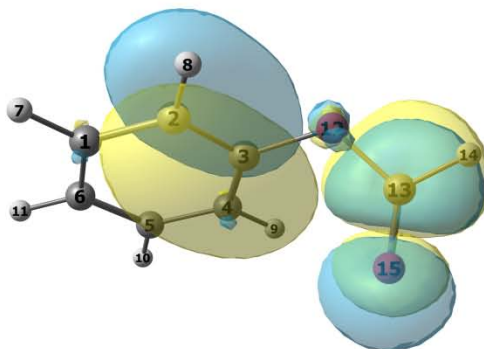
NBO deletion analysis confirms that the presence of the $n \rightarrow \pi^*$ interaction (R₄) in the cis conformer reduces the occupancy of the lone pair electrons on carbonyl oxygen (O₁₅). Thus there is a decrease of overlap between the lone pair orbital on carbonyl oxygen (O₁₅) and σ^* orbital of O₁₂-C₁₃ which favors the reduction of the C=O stretching frequency. The case I in Table S5 reveals that the deletion of the $n \rightarrow \pi^*$ interaction increases the occupancy of the carbonyl oxygen lone pair electrons. The case II demonstrates that the deletion of the R₂ interaction against the deletion of both R₂ and R₄ interactions reduces the occupancy of the carbonyl oxygen lone pair electrons.

(a)



$$C_2 = C_3(\pi^*) \text{ \& } C_{13} = O_{15}(\pi)$$

(b)



$$C_2 = C_3(\pi) \text{ \& } C_{13} = O_{15}(\pi^*)$$

Fig. S2. NBO view of (a) π^* orbital of phenyl ring and π orbital of carbonyl group and (b) π orbital of phenyl ring and π^* orbital of carbonyl group in the cis conformer of phenyl formate.

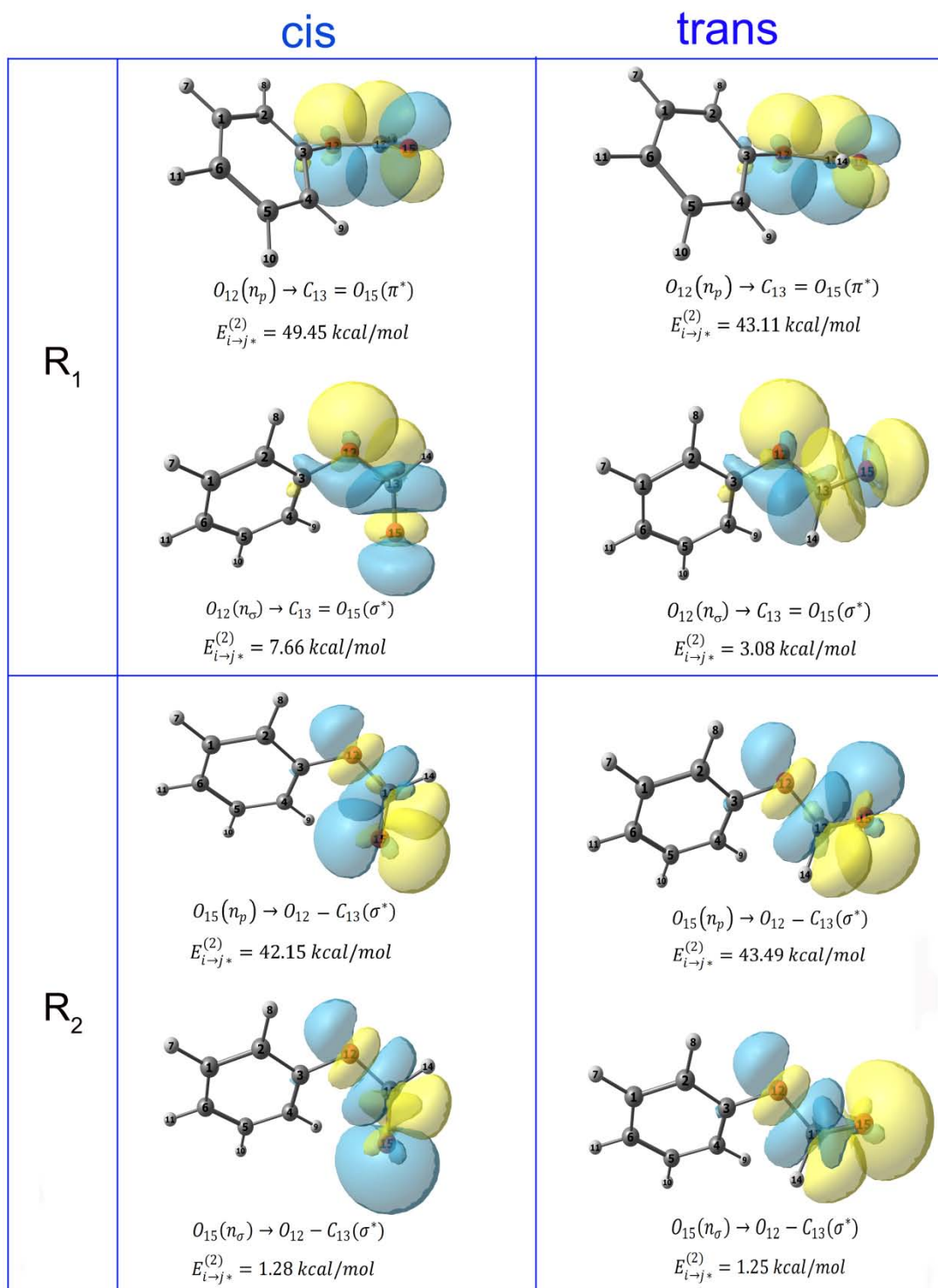


Fig. S3. NBO view for the overlap of donor and acceptor orbitals involved in R_1 and R_2 interactions in the cis and trans conformers of phenyl formate. R_1 and R_2 are defined at the footnote of Table S3.

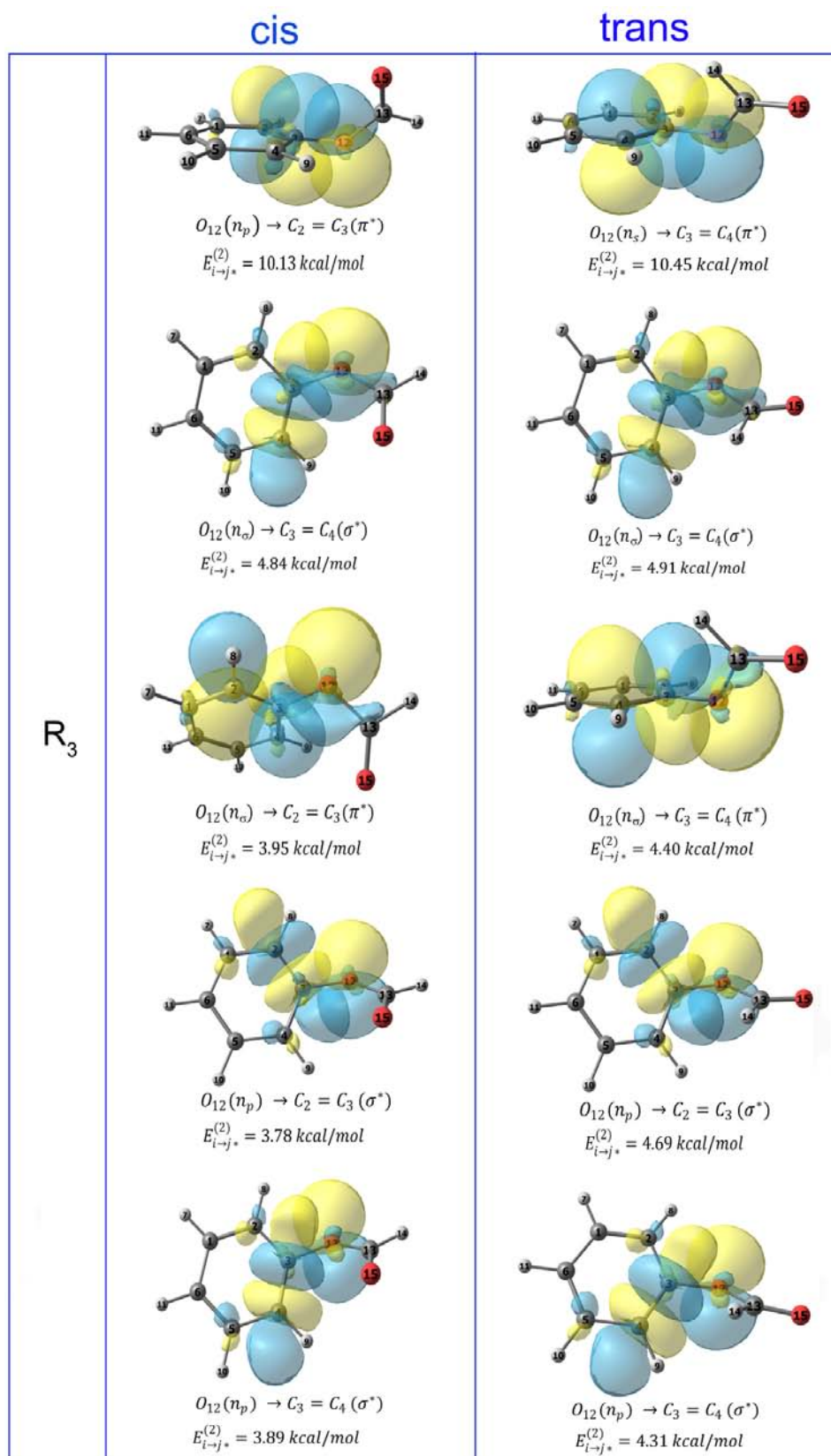


Fig. S4. NBO view for the overlap of donor and acceptor orbitals involved in R₃ interaction in the cis and trans conformers of phenyl formate. R₃ is defined at the footnote of Table S3.

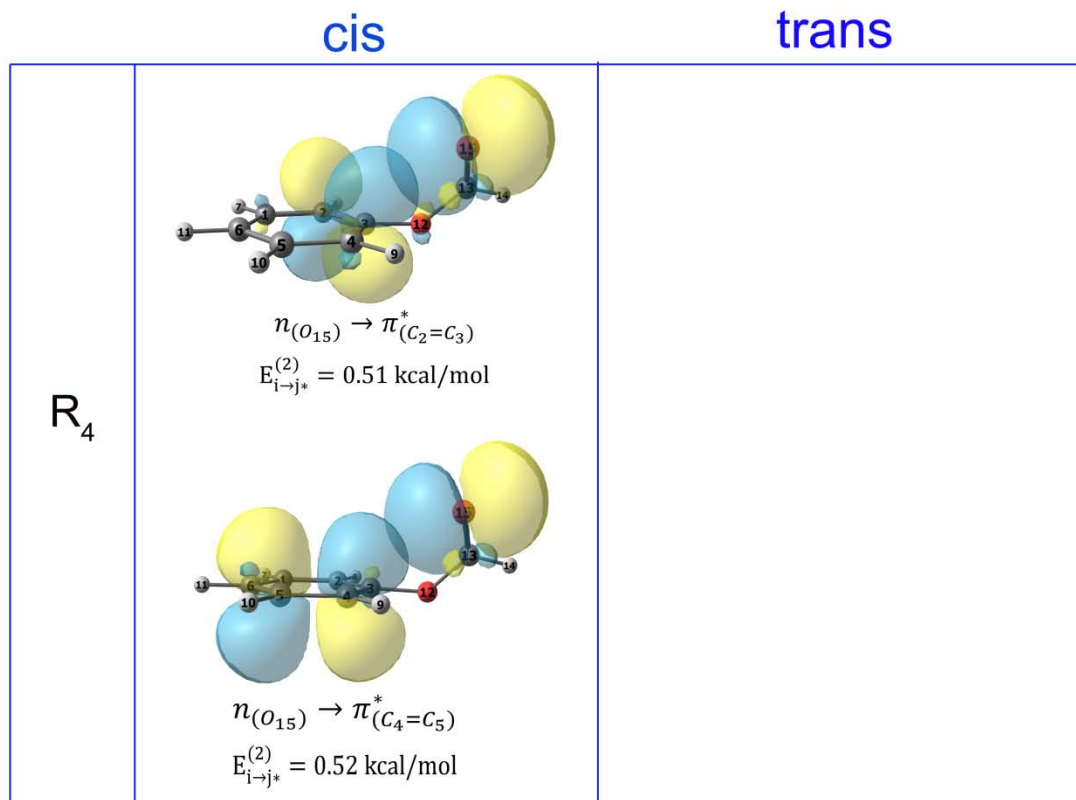


Fig. S5. NBO view for the overlap of donor and acceptor orbitals involved in R_4 interaction in the cis conformer of phenyl formate. R_4 is defined at the footnote of Table S3.

Detailed NBO analysis of phenyl formate

Wiberg Bond Index calculation shows that the bond order of C=O for the cis conformer is 1.8142 while the same for the trans conformer is 1.8388. The lower bond order of C=O for the cis conformer compared to that for the trans conformer indeed supports for the lower C=O stretching frequency in the former one relative to the latter one.

A comparison of second order perturbative energy values as well as energies of donor and acceptor orbitals for interactions between various NBOs in the cis and trans conformers of phenyl formate have been provided in Tables S3. The NBOs showing overlap between various orbitals in the cis and trans conformers of phenyl formate have been shown in Figure S3-S5.

First of all, the NBO data show that there is no significant overlap (interaction) between the π -orbitals of the carbonyl group and the phenyl ring in both the conformers of phenyl formate (See Figure S2). Interestingly, there are two opposing electronic effects which influence the carbonyl

stretching frequency in phenyl formate. One of the factors denoted by R_1 (see Table S3), which reduces the carbonyl stretching frequency or weakens the C=O bond, is the delocalization of the lone pair electrons (p-type and σ -type) on ether oxygen (O_{12}) into carbonyl π^* and σ^* orbitals ($C_{13}=O_{15}$). This is also called resonance effect. The reduction in the C=O stretching frequency will be more as the overlap between these lone pair and carbonyl π^*/σ^* orbitals increases. Another factor denoted by R_2 , which increases the carbonyl stretching frequency or strengthens the C=O bond, is the delocalization of the lone pair electrons (p-type and σ -type) on carbonyl oxygen (O_{15}) into the σ^* orbital of $O_{12}-C_{13}$. So the increase in the C=O stretching frequency will be more as the overlap between these two orbitals will be more efficient. Additionally, interaction (denoted as R_3) of the lone pair electrons (p-type and σ -type) on the ether oxygen (O_{12}) with the π^* and σ^* orbitals of the phenyl ring opposes the R_1 factor and favors the R_2 factor. R_2 factor is generally called inductive effect (here it is $-I$ effect). All of these electronic interactions are present in cis as well as trans conformer of phenyl formate. But the $n \rightarrow \pi^*$ interaction (denoted by R_4) between the lone pair electrons on carbonyl oxygen and π -cloud of the phenyl ring is present only in the cis conformer of phenyl formate but not in the trans conformer.

Combined value for multiple contributions to each of the four interactions (R_1 , R_2 , R_3 , and R_4) is listed in Table S4. A close inspection into the NBO stabilization energy values listed in Table S4 reveals that the R_1 value which favors the reduction of the C=O stretching frequency in phenyl formate is higher by 11 kcal/mol in the case of the cis conformer compared to the trans conformer. On the other hand, the R_2 and R_3 values, which support the increase of the C=O stretching frequency, are lower by 1.35 kcal/mol and 2 kcal/mol, respectively for the cis conformer in comparison to the trans conformer. Thus all these interactions favor the reduction of the C=O stretching frequency in the cis conformer compared to that in the trans conformer of phenyl formate.

The question is why the orbital interactions in the cis conformer relative to the trans conformer favor the reduction of the C=O stretching frequency. The fact is that the $n \rightarrow \pi^*$ interaction, which is present only in the cis conformer, affects the R_1 , R_2 , and R_3 interactions in favor of reduction of the carbonyl force constant in the cis conformer compared to that in the trans conformer. The $n \rightarrow \pi^*$ interaction in the cis conformer partially reduces the electron density on the carbonyl oxygen (O_{15}) and consequently this reduction in the electron density induces the enhancement in the R_1 interaction (resonance effect) i.e. overlap between the carbonyl π^* orbital and ether oxygen (O_{12}) lone pair orbital. As the lone pair electrons on ether oxygen (O_{12}) are involved more in the R_1 interaction in the cis conformer, the value of the R_3 interaction involving the same lone pair electrons decreases there.

Similarly, as the lone pair electrons on the carbonyl oxygen (O_{15}) is involved in the $n \rightarrow \pi^*$ interaction in the cis conformer, the R_2 factor i.e. the NBO stabilization energy for the interaction between the lone pair orbital on carbonyl oxygen (O_{15}) and σ^* orbital of $O_{12}-C_{13}$ is less in the cis

conformer compared to that in the trans conformer. We have performed NBO deletion analysis which clearly proves this. Table S5 shows occupancy of the lone pair electrons on the carbonyl oxygen (O₁₅) in the cis conformer with deletion of specific NBO interactions. It is intriguing to note that the occupancy of the lone pair electrons on carbonyl oxygen (O₁₅) in the cis conformer is more when the $n \rightarrow \pi^*$ interaction is deleted. As the $n \rightarrow \pi^*$ interaction reduces the occupancy of the carbonyl oxygen (O₁₅), the R₂ factor responsible for the strengthening of the C=O bond decreases in the cis conformer.

Thus it is clear that the red-shift in the C=O stretching frequency in the cis conformer of phenyl formate compared to that in the trans conformer is due to the presence of the $n \rightarrow \pi^*$ interaction, in the former one, which favors the neighboring orbital interactions which reduces the C=O stretching frequency. This observation will be true for any molecule/complex with a carbonyl group attached to a neighboring electronegative atom (O, N etc.) i.e. -HN-C=O or RO-C=O and the C=O group is involved with $n \rightarrow \pi^*$ or other non-covalent interactions.

References

- [1] S. Kumar, I. Kaul, P. Biswas, A. Das, *J. Phys. Chem. A* **2011**, *115*, 10299.
- [2] M. J. Frisch, G. W. Trucks, H. B. Schlegel, G. E. Scuseria, M. A. Robb, J. R. Cheeseman, G. Scalmani, V. Barone, B. Mennucci, G. A. Petersson, H. Nakatsuji, M. Caricato, X. H. Li, H. P., A. F. B. Izmaylov, J., G. Zheng, J. L. Sonnenberg, M. Hada, M. Ehara, K. Toyota, R. Fukuda, J. Hasegawa, M. Ishida, T. Nakajima, Y. Honda, O. Kitao, H. Nakai, T. Vreven, J. Montgomery, J. A., J. E. Peralta, F. Ogliaro, M. Bearpark, J. J. Heyd, E. Brothers, K. N. Kudin, V. N. Staroverov, R. Kobayashi, J. Normand, K. Raghavachari, A. Rendell, J. C. Burant, S. S. Iyengar, J. Tomasi, M. Cossi, N. Rega, N. J. Millam, M. Klene, J. E. Knox, J. B. Cross, V. Bakken, C. Adamo, J. Jaramillo, R. Gomperts, R. E. Stratmann, O. Yazyev, A. J. Austin, R. Cammi, C. Pomelli, J. W. Ochterski, R. L. Martin, K. Morokuma, V. G. Zakrzewski, G. A. Voth, P. Salvador, J. J. Dannenberg, S. Dapprich, A. D. Daniels, Ö. Farkas, J. B. Foresman, J. V. Ortiz, J. Cioslowski, D. J. Fox, *Gaussian 09, Revision B.01*, Gaussian, Inc., Wallingford CT (2009)
- [3] E. D. Glendening, A. E. Reed, J. E. Carpenter, F. Weinhold, in *NBO Version 3.1*, online at http://www.gaussian.com/g_tech/g_ur/m_citation.htm